The Use of Biochar and Pyrolysed Materials to Improve Water Quality through Microcystin Sorption Separation

Vladimír Frišták [1,*] [ID]**, H. Dail Laughinghouse IV [2]** [ID] **and Stephen M. Bell [3]** [ID]

[1] Department of Chemistry, Trnava University in Trnava, 91843 Trnava, Slovakia
[2] Fort Lauderdale Research and Education Center, Agronomy Department, University of Florida/IFAS, Davie, FL 33314, USA; hlaughinghouse@ufl.edu
[3] Institute of Environmental Science and Technology (ICTA-UAB), Universitat Autónoma de Barcelona, 08193 Barcelona, Spain; Stephen.Bell@uab.cat
* Correspondence: fristak.vladimir.jr@gmail.com; Tel.: +421-33-592-1459

check for updates

Abstract: Harmful algal blooms have increased globally with warming of aquatic environments and increased eutrophication. Proliferation of cyanobacteria (blue-green algae) and the subsequent flux of toxic extracellular microcystins present threats to public and ecosystem health and challenges for remediation and management. Although methods exist, there is currently a need for more environmentally friendly and economically and technologically feasible sorbents. Biochar has been proposed in this regard because of its high porosity, chemical stability, and notable sorption efficiency for removing of cyanotoxins. In light of worsening cyanobacterial blooms and recent research advances, this review provides a timely assessment of microcystin removal strategies focusing on the most pertinent chemical and physical sorbent properties responsible for effective removal of various pollutants from wastewater, liquid wastes, and aqueous solutions. The pyrolysis process is then evaluated for the first time as a method for sorbent production for microcystin removal, considering the suitability and sorption efficiencies of pyrolysed materials and biochar. Inefficiencies and high costs of conventional methods can be avoided through the use of pyrolysis. The significant potential of biochar for microcystin removal is determined by feedstock type, pyrolysis conditions, and the physiochemical properties produced. This review informs future research and development of pyrolysed materials for the treatment of microcystin contaminated aquatic environments.

1. Introduction

Recent studies indicate that cyanobacterial harmful algal blooms (cyanoHABs) are occurring more frequently in inland fresh waters (i.e., ponds, lakes, streams, and rivers) and estuaries worldwide [1–4]. Higher temperatures linked to global climate change and increased eutrophication have intensified cyanoHABs, posing significant environmental, social, and economic impacts partly due to the effects of toxins produced by several taxa [5–8]. Monitoring toxicity following such events in waterbodies can be complicated as cyanobacterial blooms contain complex mixtures of different classes of toxins [9–11]. Nevertheless, increased research efforts on the toxic impacts of these blooms under a changing climate and practical tools and methods for their management and remediation are clearly needed [4–14].

Microcystins (MCs) are a group of naturally occurring toxic secondary metabolites (cyanotoxins) produced by various genera of cyanobacteria [9–15]. They can be fatal to freshwater organisms even at very low concentrations [5–16] and have been classified by the International Agency for Research on Cancer (IARC) as possible human carcinogens [17]. To meet World Health Organization

(WHO) guidelines for maximum allowed surface water concentrations [18], there are several processes available for the removal of extracellular MCs. Powdered and granular activated carbon are commonly applied to adsorb MCs during treatment processes of drinking water because of their unique sorbent characteristics [19–21]. However, production costs for activated carbon and other materials (e.g., carbon nanotubes) have limited their potential for widespread application [19–22].

There is a current demand for more environmentally friendly and economically and technologically feasible sorbents for water quality remediation to be used in tandem with bloom prevention and risk reduction [23]. Pyrolysis, the thermochemical conversion of organic matter into char under anoxic or low-oxygen conditions, is a cheap and attractive method for the production of new sorption materials for water treatment purposes [24,25]. As a product of pyrolysis, biochar is of interest in this regard owing to the possibility of specifically designing, through feedstock and production process manipulation, more efficient sorption properties [26]. The high porosity, chemical stability, and significant sorption efficiency for removing cyanotoxins are among the central advantages of biochar [25]. In aqueous solutions, biochar and modified charcoal have provided promising results as sorbents [27–29], however, existing knowledge gaps have hindered widespread application in water treatment processes.

To address the need for an updated review of microcystin removal strategies, this paper first provides an overview of microcystin toxicity in natural water bodies followed by a discussion on conventional and alternative sorbents for microcystin separation. Here, this review focuses on the most pertinent chemical and physical sorbent properties responsible for effective removal of various pollutants from wastewater, liquid wastes, and aqueous solutions. Furthermore, an in-depth assessment of the pyrolysis process for sorbent production is given, providing the first comprehensive evaluation of biochar as a sorbent for microcystin removal. This review informs future research and development of pyrolysed materials for the treatment of microcystin in aquatic environments.

2. Microcystin Origin and Toxicity in Natural Water Bodies

Cyanobacteria are oxygenic photosynthetic bacteria that are prevalent in nutrient rich, warm, low turbulent freshwater bodies. When cyanobacteria die, their cell walls degrade, releasing intracellular toxins into the surrounding aquatic environment. MCs are a group of these naturally occurring toxins produced by various genera of cyanobacteria (e.g., *Anabaena*, *Anabaenopsis*, *Aphanocapsa*, *Cyanobium*, *Dolichospermum*, *Hapalosiphon*, *Limnothrix*, *Microcoleus*, *Microcystis*, *Nostoc*, *Oscillatoria*, *Phormidium*, *Planktothrix*, *Pseudanabaena*, *Sphaerospermopsis*, and *Synechocystis*). Their structures are extremely stable in water and can withstand chemical breakdown such as hydrolysis or oxidation. From a chemical point of view, MCs represent cyclic peptides composed of five common amino acids and pairs of L-amino acids as variants [30]. The common ones are D-erythro-β-methylaspartic acid, alanine, *N*-methyldehydroalanine, glutamic acid, and a unique amino acid called Adda (3-amino-9-methoxy-2,6,8-trimethyl-10-phenyldeca-4,6-diene acid). There have been more than 240 variants of MCs reported [31,32].

The main structural differences between microcystin variants arise from the substitution of single amino acids (Figure 1). In MC-LR, the most toxic and abundant microcystin, the two variable L-amino acids are L-arginine and L-leucine [33]. Trinchet et al. [34] and Roegner et al. [23] highlighted preferential organ uptake, and thus the importance of other congeners such as MC-RR (arginine at positions 2 and 4), MC-LA (leucine and alanine), MC-YR (tyrosine and arginine), MC-LF (leucine and phenylalanine), and MC-LW (leucine and tryptophan). The WHO established the guideline of a maximum recommended concentration of 1 μg/L for MC-LR in surface water. However, there remains a lack of data with respect to other structures and metabolites. According to the IARC, MCs are placed into group 2B as possible human carcinogens [17]. They are classified as tumour initiators with DNA-damaging effects [35]. These heptapeptides are produced via a nonribosomal biosynthesis pathway by large multienzyme complexes that include peptide synthetases, polyketide synthases, and tailoring enzymes [36].
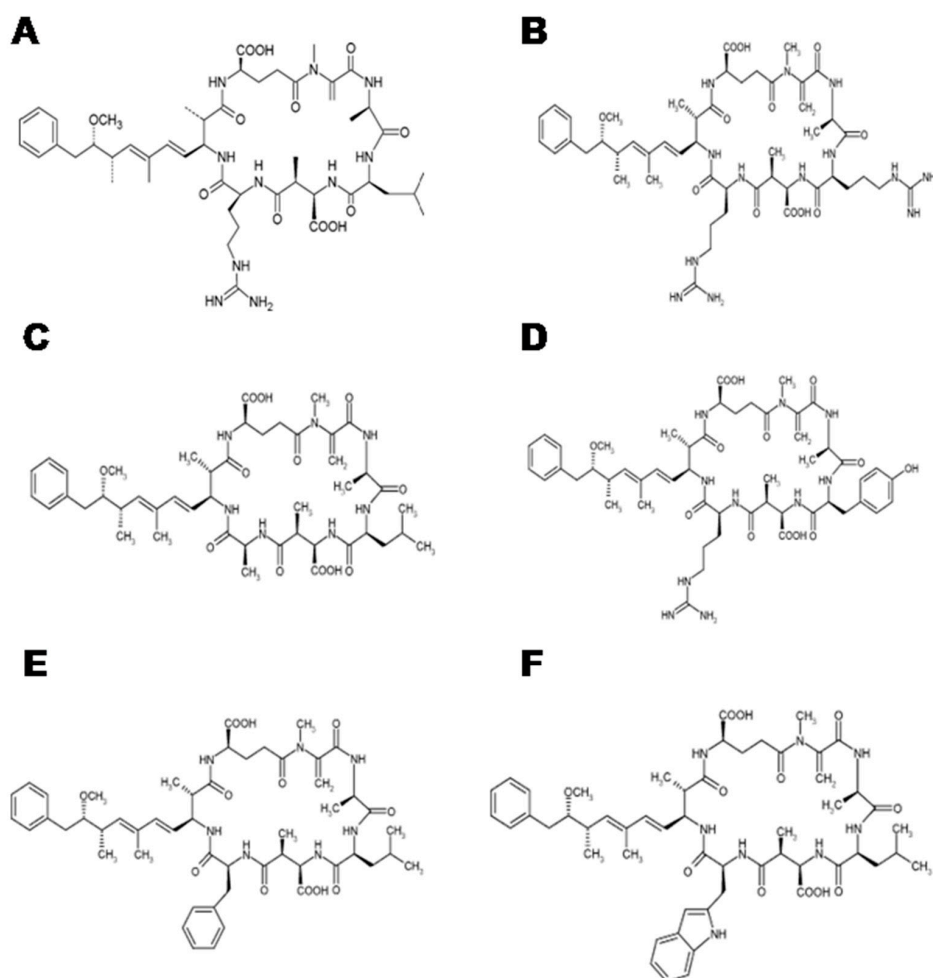
Figure 1. (**A**) Chemical structure of microcystin (MC)-LR, (**B**) microcystin-RR, (**C**) microcystin-LA, (**D**) microcystin-YR, (**E**) microcystin-LF, and (**F**) microcystin-LW.

In active and growing cyanobacteria, most MCs are cell-bound with intracellular concentrations of MCs several orders higher than concentrations of dissolved MCs in water. However, bloom senescence and cell lysis can cause the release of high quantities of MCs into the water. Mazur-Marzec et al. [37] and Jones et al. [38] reported that MC-LR can persist in aquatic for 1–3 months, but this is dependent on limnological and environmental parameters [39]. Based on acute toxicity, MC-LR is considered one of the most significant cyanobacterial toxins. As hepatotoxins, MCs mainly affect liver functioning, and can cause mortality and morbidity through necrosis and haemorrhage [40]. The hydrophilic characteristic of most MCs facilitates its uptake in vertebrates via active transport compared with cell membranes [41]. Membrane transport occurs mainly via organic anion transporting polypeptides [42].

Inside the hepatocytes, MCs inhibit eukaryotic protein serine/threonine phosphatases 1 and 2A [41], resulting in cytoskeletal disruption, rearrangement of associated filamentous actin, and morphological changes [23]. Frangez et al. [43] confirmed covalent binding of microcystin structure to protein phosphatases, leading to hyperphosphorylation of cytoskeletal proteins and the disruption of many cellular processes. Davis et al. [44] showed the effect of MC-LR on activation of the mitogen-activated protein kinase pathway. MCs induce apoptosis through free radical formation and mitochondrial alternations [23–45]. Human health problems are mostly related to chronic exposure to MCs via food and water consumption. As tumor-promoting toxins, MCs alter the regulation of phosphorylation and induce DNA damage in hepatocytes [46].

3. Conventional Strategies of Microcystin Removal

The removal or inactivation of MCs from water can be affected by several factors. The most crucial among these is if MCs are concentrated extracellularly or intracellularly. As mentioned, the majority (>95%) of MCs are found intracellularly during the growth stage of the bloom. However, when blooms collapse as a result of nutrient depletion, high temperatures, viral attack, and/or through the effect of chemical agents, intracellular MCs are released into the water as extracellular, increasing dissolved microcystin concentrations. The most common processes of extracellular MCs removal from drinking water are divided into three general steps: physical removal, biological inactivation, and chemical inactivation. Very often, these steps are cross-linked and supplied by processes such as sedimentation and flocculation. Physical removal includes the adsorption by effective sorbents (usually activated carbon) and the application of several filtration techniques [47,48]. Conventional sand filtration may be sufficient, but could also enhance the release of high concentrations of MCs into treated water [49,50]. Suboptimal set-up of filtration parameters, such as flow rate, can very often lead to enormous leaching of MCs from lysed microbial cells.

The main objective of the traditional sequence of coagulation–sedimentation–flocculation processes is to remove live algae, their residues, and organic and inorganic matter. A potential side-effect is cell lysis and subsequent increases in dissolved cyanotoxins' (e.g., MC) concentrations. The character and properties of cyanobacterial organic matter and toxic compounds decrease the efficacy of the conventional process for inorganic substances. Roegner et al. [23] described in detail the main disadvantages and pitfalls of the coagulation–sedimentation system when applied for MCs removal. Teixeira and Rosa [51] highlighted the significant effect of local water quality on MCs removal by this conventional method. Additionally, the quantity and quality of the chemical coagulant represents an important factor in the removal process. The application of flotation, a process whereby solids in suspension are recovered by their attachment to gas (usually air) bubbles, in combination with coagulation and flocculation, shows positive results in MCs separation [52]. The particles most effectively removed are in the size range of 10–200 μm. The particle-bubble aggregates that are formed have a density less than the suspension itself and they rise to the surface to be removed. Despite the high efficiency of this technology for algal residues removal, the question of extracellular toxins removal is still quite open. Therefore, the application of other methods is still needed.

From a treatment standpoint, MCs have three general areas subject to oxidation: the conjugated double bond in the Adda moiety; the single double bond in the Mdha moiety; and the side chain of amino acids [47]. Laszakovits and MacKay [53] described in detail the removal of cyanotoxins by potassium permanganate. However, this method represents a pH dependent and chemically demanding process. Several studies exist on verifying the efficiency of registered chemical algaecides and herbicides (especially copper-based and peroxide-based products) for bloom treatment and MC removal [54–56]. These compounds have been used successfully for decades, but initial cyanobacterial cell and toxin concentrations, algal species, and limnological characteristics can affect efficacy. Further, usage of waters (e.g., recreation vs. drinking water) and local regulations must be considered before application. Brooke et al. [57] showed reduced concentrations of MC-LR in water after ozone application. However, this pH dependent process is less effective under alkaline conditions. Chlorination can be viewed as another potential method to remove cyanotoxins from aqueous solutions [58]. Oxidation, chlorination, and ozonization can bring new risk such as secondary pollution from their by-products. Lawton et al. [59] showed the application of ultraviolet radiation as an effective, but expensive method to remove MCs from water.

Activated carbon produced from different precursor feedstocks such as coal or coconut represents the main sorption material used in separation processes of MCs from aqueous solutions [20–60]. The surface characteristics and pore structure of activated carbon determine its range of applicability in purification technologies of polluted water [61]. The activation process affects the adsorptive capacity, which can vary and only be effective for a specific group of contaminants. Activated carbon removes

MCs mainly via mechanisms of adsorption and intraparticular diffusion [62,63]. MCs primarily interact with carbon surfaces by hydrophobic forces and electrostatic interactions [64].

Generally, two basic types of activated carbon, powdered activated carbon and granular activated carbon, are applied in treatment processes for drinking water. The main difference in use is based on type and character of the contaminant (synthetic/natural, inorganic/organic). Porosity (total pore volume), porous character, and surface characteristics are crucial for efficiency of MCs sorption. Activated carbon provides a system of micropores with diameters of <2 nm, mesopores with diameters from 2 to 50 nm, and macropores at >50 nm. Microporous filtration materials restrict water flow and reduce contact between MCs and active surface sites, and thus can be considered as less effective in the removal process. On the other hand, MCs can be easily separated by activated carbon with high concentrations of mesopore structures [64].

Researchers have confirmed the different sorption efficiencies of activated carbons for MC-LR compared with MC-RR, MC-YR, and MC-LA. Mesoporous carbon materials with targeted functional groups represent an option in MCs separation from aqueous solutions [65]. Granular activated carbon is very often used in fixed beds as a filtration medium or adsorbent to remove fragile particles and chemicals under continual flow conditions [47]. However, Newcombie et al. [66] showed the inefficiency of granular activated carbon-based filters for microcystin separation compared with granular activated carbon-based adsorbents with proper regeneration or replacement, which can be potentially used as auxiliary barriers. Ho and Newcombie [67] found that powdered activated carbon can be easily bound up in the floc structure during the coagulation process, and thus can reduce the efficiency of MCs removal. Roegner et al. [23] showed the importance of the activated carbon's feedstock on the removal efficiency of MCs from potable water. The authors summarized that activated carbon produced from wood contains a system of mesopores and micropores, while coconut-based activated carbon contains just micropores, which can limit its MCs sorption application. Hena et al. [63] described the sorption process of MC-LR by activated carbon prepared from rubber wood sawdust as pH dependent with a maximal sorption capacity of 296 mg/g.

The effect of feedstock pH and the value of the point of zero charge (pHzpc) can significantly affect the adsorption efficiency of MCs [68]. Huang et al. [69] showed the relation between the pHzpc of activated carbon and sorption process of cyanotoxins. The higher pHzpc of the feedstock results in a neutral or positive charge of the produced activated carbon and higher adsorption potential for MCs [23]. The efficiency of activated carbon and activated carbon-based filters in separation of MCs from drinking water is considered sufficient (>99%) [70]. However, concentrations of cyanotoxins in water are potentially low and filters are not typically challenged with higher doses or the competitive effect of other toxic agents. Chlorine pre-treatment of potable water presents a problem for MCs sorption separation efficiency related to the reaction between residual chlorine and active carbon sites. Another problematic issue of causing a decrease in sorption separation with activated carbon application in water can be high concentrations of organic matter. Natural organic matter competes simultaneously with MCs for active sorption sites on surfaces of activated carbon.

Granular activated carbon can additionally be used as an ideal habitat for microbial growth thanks to its large surface area [47]. The growth of different microorganisms on activated carbon-based filters and biofilm formation can enhance the MCs removal owing to the combined effect of MCs biological degradation and sorption separation [69]. On the other hand, biofilm formation can decrease pore availability and thus reduce separation efficiency [23]. Drogui et al. [71] showed the lower efficiency of activated carbon-based filters after colonization by microbial communities compared with sterile filters during separation of MC-LR from water. The concerning literature discrepancies in the assessment of microbial colonization on MCs separation by activated carbon require additional and more detailed studies.

Numerous research studies refer to the decrease in accessibility and increase in mass production costs of activated carbon derived from typical feedstocks such as coal, coconut, or wood [19–22]. Zhi et al. [72] reported a price of 1650–9900 USD/t for activated carbon for pollutant removal,

while Lou et al. [73] determined a range of 20,000–80,000 USD/t for carbon nanotubes. Based on these assessments, more economical and environmentally friendly sorbents are needed for water quality control.

4. Alternative Microcystin Separation Sorbents

Conventional technologies of MCs removal from water can be expensive and very often simply insufficient. More affordable methods with low technological requirements in water treatment are needed according to Gurbuz and Codd [50]. The authors highlighted a number of natural and artificial materials with extensive internal porosity for application in water purification. Despite possessing a lipophilic side chain of ADDA residue, molecules of microcystins are quite hydrophilic because of two carboxylic groups on its aspartic/glutamic acid side and one guanidine group on its arginine acid side [74]. Kim et al. [75] applied industrial waste biomass of *Escherichia coli* to develop biosorbents for MC-LR immobilization. The authors created biomass stabilization with polysulfone, coating the polysulfone-biomass composite with polyethylenimine, and subsequent decarboxylation of coated material. Such prepared materials can be recommended as highly efficient sorbents for MC-LR removal from aquatic environments with maximum sorption capacities of 1.2–1.9 mg/g at approximately pH 5. MC-LR can be effectively removed from aqueous solutions by sorbents prepared from *Moringa oleifera* Lam. seeds, as shown by Yasmin et al. [76]. The authors applied an acid pre-treatment of seed powder to increase pore size and volume. The sorption capacity of modified biosorbent for MC-LR was >92 mg/g. Sathya et al. [77] applied an exocellular polymer from *Enterobacter ludwigii* to remove microcystin-RR extracted from *Microcystis aeruginosa* (Kützing) Kützing. The maximum removal of MC-RR by the studied polymer was optimized by response surface methodology and achieved at a contact time of 5 h, pH 10, temperature of 30 °C, agitation speed of 150 rpm, and polymer dose of 4 mg/mL. This study confirmed the removal efficiency of MC-RR by exocellular polymer with a maximum sorption capacity of 23.76 ng/mg. Additionally, the authors showed a positive effect of Cu^{2+} ions on the MC-RR removal process by microbial polymeric material.

Application of native or dried biomass to separate MCs from aqueous solutions can cause secondary contamination by releasing other polymeric substances of heterogeneous composition into purified solution. The instability of biomass-derived sorbents represents a hazardous point that has to be mentioned [78]. Therefore, inorganic and thermochemically transformed materials are a more promising choice [79]. Morris et al. [80] showed high efficiency (>80%) of MC-LR separation from water by naturally-occurring clay particles. Laughinghouse et al. [81] found that lanthanum modified bentonite clay was able to sediment MC-LR at higher concentrations (around 500 µg/L) when compared with lower concentrations (50 and 100 µg/L). Adsorption of MC-LR onto nano-sized montmorillonite was investigated and optimized by Wang et al. [82]. Their work indicated a pH dependent process with the maximum of 0.186 mg/g reached at pH 2.96. Removal of MC-LR from model aqueous solutions by nano-sized montmorillonite represents a rapid process with several kinetic stages. Desorption efficiency of sorbed MC-LR (>75%) can be reached using 0.1 mol/L NaOH as the eluting media. Superabsorbent polymer composites appear to be a cost-effective solution for MC-LR adsorptive removal [83]. The porous network structure and the ionic functional groups of superabsorbent polymers ensure diffusion and binding of microcystin molecules. Wang et al. [83] showed the effective application of polyacrylamide/sodium alginate-modified montmorillonite to remove MC-LR from aqueous solution. Their study described sorption as a fast process, reaching equilibrium within 80 min of contact time. The maximum adsorption capacity of polyacrylamide/sodium alginate-modified montmorillonite for MC-LR was 32.66 mg/g. The authors also discovered that over 85% adsorption and 80% desorption could be achieved after five regeneration cycles. Recovery of studied microcystin reached more than 92% without ionic effect.

The sorption potential of pumice for MCs has also been described by Gurbuz and Codd [50]. Pumice is a porous material with high numbers of active sites that can be used as effective filtration material. The application of pumice in slow filtration processes to remove pathogens from irrigation

water is a well-known method in horticulture [84]. Gurbuz and Codd [50] showed MC-LR adsorption on a pumice-based sorbent as a pH dependent process with maximal efficiency at pH 4. Experimental studies on the removal of MC-LR by peat showed the important role of this biomaterial in separation processes of cyanotoxins [85]. The maximum adsorption capacity of peat for MC-LR was found to be 0.26 mg/g at pH 3. Regeneration of peat-based sorbent using 2 mol/L NaOH showed a 94% efficiency in MC-LR desorption.

Iron oxides and hydroxides influence the mobility of organic and inorganic compounds in soils, sediments, and surface water. Therefore, Lee and Walker [86] studied the potential of maghemite nanoparticles to adsorb MC-LR from model solutions and confirmed a strong effect of pH with maximum removal efficiency at pH 3. They described the electrostatic interactions and hydrophobic forces as being crucial MC-LR sorption mechanisms. The adsorption process of microcystin onto maghemite nanoparticles is not significantly affected by the presence of river fulvic acid at lower concentrations (<2.5 mg/L). At higher concentrations of fulvic acid, the adsorption process of MC-LR by iron oxide nanoparticles decreased as a result of competition for limited active sorption sites. Along similar lines, Okupnik et al. [87] investigated the use of titanium dioxide nanoparticles for removal of MC-LR in environmental relevant concentrations from water samples. The authors tested different crystalline phases of nano-TiO_2 such as anatase, rutile, and an anatase–rutile mixture in comparison with a bulk TiO_2 counterpart. Sorption separation of MC-LR by titanium dioxide nanoparticles represents a complex mechanism, with chemisorption and sorbent particle size as the most influencing factors. Kinetic and equilibrium results of microcystin-LR and microcystin-RR removal by graphene oxide from water polluted by other environmental co-pollutants were described in a study by Pavagadhi et al. [61]. The tested graphene oxide showed significant adsorption capacity at 1.70 mg/g for MC-LR and 1.88 mg/g for MC-RR even in the presence of Mg^{2+}, Ca^{2+}, K^+, and Na^+ cations and NO^{2-}, NO^{3-}, Cl^-, SO_4^{2-}, and PO_4^{3-} anions. The sorption kinetic experiments revealed that more than 90% removal of both microcystin variants is achieved within the first 5 min. New sorbents based on N-doped carbon xerogel for MC-LR adsorption were synthesized by Wu et al. [88]. Their results indicate fast microcystin uptake within 10 min and an adsorption capacity of 1.92 mg/g. The authors highlighted the efficiency of sorbent regeneration using 1 mol/L NaOH applied as the desorption agent.

5. New Sorption Materials Produced with Pyrolysis

Various feedstocks can be thermochemically converted into char using carbonization processes such as torrefaction, pyrolysis, hydrothermal carbonization, or gasification. Pyrolysis proceeds under strict anoxic or low oxygen conditions at temperatures from 350 to 1000 °C, and it is the main carbonization technique to produce conventional biochar with required characteristics [89]. During the pyrolysis process, solid (char), liquid (condensable crude oil), and gaseous (non-condensable syngas) products are formed. The solid products of hydrothermal carbonization, torrefaction, or gasification do not fulfil the main definition of biochar. According to Shaheen et al. [90], pyrolysis represents a less expensive and more robust technology involving thermochemical decomposition of organic matter compared with the other methods mentioned.

The physical and chemical characteristics of biochar are fully dependent on the feedstock properties and production system (Figure 2) [91]. The European Biochar Certificate outlines a wide range of biomass feedstocks approved for use in biochar production [89]. Biomass can be sourced through local waste collection services following waste separation (biodegradable wastes), garden waste (leaves, flowers, roots, hay, grass, prunings from trees, vines, bushes), agriculture and forestry (harvest leftovers, straw, husks and grain dust, seeds, plants, bark and chippings, sawdust, wood, wool), animal by-products (bones, manure, skins, hairs, feathers), material from food and confectionary production (leftovers from the production of canned food; residues from potato, rice, or corn starch production; residues from dairy processing; tobacco dust; slacks; ribs; tea; and coffee grounds), textiles (cellulose, cotton fibres, wool leftovers, hemp), or biogas plants (fermentation residues). Additionally, there exist

several approved mineral-organic additives such as lime, bentonite, clay, loam, rock flour, or lignite to improve pyrolysis conditions and, subsequently, the quality of the produced biochar.
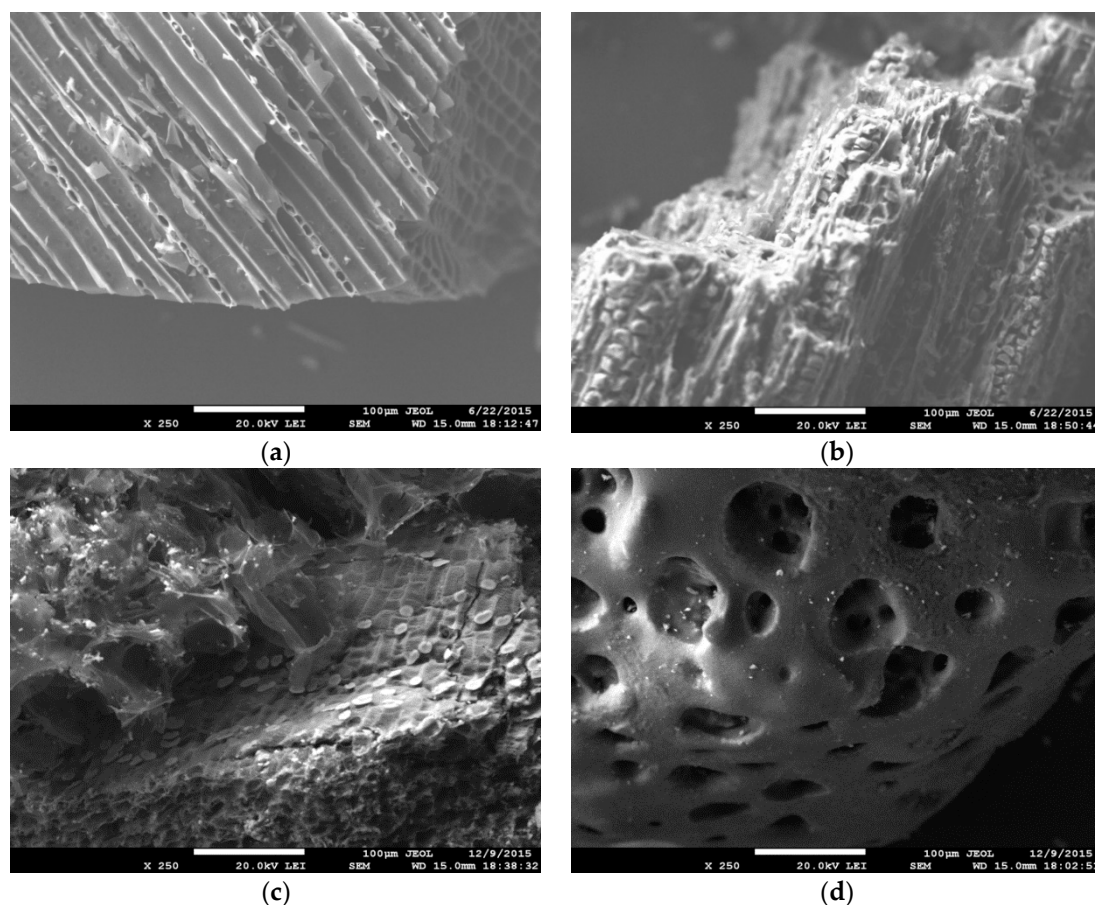

Figure 2. Scanning electron microscopy (SEM)—images of biochar derived from wood chips (**a**), garden green waste (**b**), corn cobs (**c**), and sewage sludge (**d**) at magnification 250× (with permission of authors—Michaleková-Richveisová et al. [91]).

Pyrolysis usually includes slow, fast, and flash processes [25]. Slow pyrolysis (conventional carbonization) is characterized by feedstock placement into a reactor and then initiating heating at a rate of about 0.1–1 °C/s until achieving a residence time from 20 min to several hours at temperatures of 400–700 °C. This process produces a solid char product rather that crude oil and syngas. While for fast and flash pyrolysis, addition of feedstock into the reactor occurs after pyrolysis temperature has been reached, with a significantly reduced residence time of several seconds to a few minutes at temperatures from 500 to 800 °C [92]. Fast pyrolysis produces a major bio-oil fraction and minor biochar and syngas by-products [93].

The fibrous biomass consists of cellulose, hemicelluloses, and lignin with smaller quantities of organic extractives and inorganic minerals. These constituents vary among different kinds of biomass. Cellulose as a linear condensation polymer of β-(1–4)-ᴅ-glucopyranose creates sheets of glucopyranose rings lying in a plane with successive sheets stacked on top of each other to form three-dimensional particles that aggregate into an elementary crystalline micro-fibril arrangement. This makes cellulose more thermal and chemically resistant compared with hemicellulose. Hardwood materials are rich in xylans and poor in glucomannans, while softwood feedstock contains more glucomannans compared with xylans [94]. Cellulose, hemicelluloses, and lignin have distinctive thermal decomposition behaviours that depend upon heating rates. Hemicellulose is the first to decompose, beginning at 220 °C and completed at 315 °C [94]. Cellulose does not start to decompose until about 315 °C.

Although lignin begins to decompose at 160 °C, it is a slow process extending to 850–900 °C. Pyrolysis of hemicellulose produces mainly no-condensable gases (CO, CO_2, H_2, and CH_4) and low molecular weight organic compounds such as carboxylic acids, alkanes, esters, and aldehydes [95]. Cellulose is a main source of considerable biochar product and the product of cellulose decomposition can vary depending on reaction conditions. The process of decomposition includes an exothermic and endothermic pathway. The exothermic pathway via anhydrocellulose yields char and non-condensable gases, while the endothermic pathway via levoglucosan is a devolatization process leading to tarry vapours or char. Mohan et al. [96] described the extent of secondary reactions affected by temperature, residence time, and catalysts occurring in feedstock. They yield a wide range of organic compounds such as carboxylic acids, ketones, aldehydes, and alcohols. The pyrolysis products of cellulose are mainly in the form of solid C, CO_2, and H_2O [97].

Many scientific studies focus on the utilisation of biochar and pyrolysis carbonaceous materials as effective sorbents in processes of organic and inorganic pollutant removal from aqueous solutions (Table 1). Several authors have confirmed different effects of physical and chemical properties on sorption efficiency. Therefore, the major material properties responsible for effective removal of various pollutants from wastewater, liquid wastes, and aqueous solutions are reviewed below.

Table 1. Removal of inorganic and organic pollutants from aqueous solutions by biochar.

Pollutant	Feedstock	Pyrolysis Temperature (°C)	Initial Concentration (mg/L)	Removal Efficiency (%)	Reference
copper	macroalga	500	10	80	[98]
cadmium	rape straw	600	20	100	[99]
lead	celery	500	400	98	[99]
zinc	wheat straw	650–700	100	100	[100]
chromium	rice husk	450–500	100	100	[101]
arsenic	sewage sludge	300	0.09	53	[102]
nickel	sewage sludge	600	30	26	[103]
tetracycline	sewage sludge	800	200	60	[104]
methylene blue	mangosteen peel	800	50	80	[105]
ibuprofen	wood chips	550	2	6	[106]
atrazine	cornstraw	500	30	100	[107]
sulfamethazine	cucumber	700	50	95	[108]

The area of internal and external surfaces, commonly called specific surface area (SSA), represents a crucial physical characteristic of pyrogenic carbonaceous material. Its value is the result of feedstock quality and production conditions (i.e., pyrolysis temperature, residence time, presence of catalysts, pre-treatment of feedstock or post-treatment of biochar). SSA determination for carbon-based sorbents involves mainly N_2 or CO_2 adsorptions followed by the Brunauer–Emmett–Teller (BET) equation application.

The method of SSA determination by liquid N_2 adsorption on biochar surface at a lower temperature (77 K) indicates the total specific surface area [109]. The method of CO_2 adsorption at a relatively high temperature (273 K) reflects the surface area of pores < 1.5 nm [110]. Micháleková-Richveisová et al. [91] and Dieguez-Alonso et al. [110] discussed the effect of pyrolysis temperature on porous structure formation and thus surface area development. Zama et al. [111] produced biochar from *Morus alba* at temperatures of 350 °C and 550 °C and confirmed more than 3.5 times higher SSA at the higher temperature. The effect of feedstock on SSA of biochar is also worth addressing. Jiang et al. [112] discussed the differences in surface areas of biochars prepared from pine wood and jarrah wood. Micháleková-Richveisová et al. [91] compared three biochars from different woody and agricultural wastes and found SSA values in the range of 16–26 m^2/g for the biochars with particle sizes of 0.5–1 mm. The effect of biochar post-treatment and feedstock pre-treatment can also significantly change SSA values of the resulting products [90].

Biochar pH ranges from 5 to 11 based on the feedstock and pyrolysis temperature [97]. There is a linear correlation between pH and pyrolysis temperature. Biochar produced at temperatures

between 300 and 400 °C has a lower pH compared with biochar produced from the same feedstock at temperatures of 400–700 °C. Zhang et al. [29] explained the more alkaline pH of biochars produced at higher temperatures as a result of volatile organic compound losses and increases in basic cations. The lower pH values can be attributed to insufficient pyrolysis of material, biomass residues, and thus content with higher concentrations of phenolic and carboxylic functional groups. Elemental composition can be responsible for hydrophobicity and polarity of biochar, which can affect the contact of the material with the aqueous solution. The O/C molar ratio is used to estimate the hydrophilic nature of biochar and denote polar group concentrations in pyrogenic materials derived from carbohydrates in feedstock. The molar ratio of H/C can describe the degree of biochar carbonisation. Low values of H/C indicate a lower amount of non-carbonized biomass and thus a higher degree of carbonization [113].

The increased total content of elements such as K, Fe, Ca, Mg, and Mn can be attributed to higher concentrations of responding minerals, oxides, or oxohydroxides, which represent potential active sorption sites for pollutants removal [114]. Additionally, concentrations of surface functional groups such as carboxylic, hydroxyl, amino, phenolic, and lactic can be crucial for biochar assessment as effective sorption material. During pyrolysis under increasing temperature, most functional groups of feedstocks are lost. Kloss et al. [113] compared FT-IR spectra of biochars produced at different temperatures and found a decreased intensity of peaks corresponding to carboxylic and hydroxyl groups in samples produced at a higher temperature. Li et al. [115] applied ^{13}C NMR to investigate functional groups of rice straw and bran derived biochars produced at 100–800 °C. The authors confirmed the decreased content of aliphatic O-alkylated carbons and dominant aromatic structures in materials produced at temperatures > 300 °C.

Based on the type of contaminants, different mechanisms of sorption interactions can be proposed [116,117]. Sorption mechanisms of metals by biochar are fully dependent on the pH of the reaction solution, DOC, and competing elements concentrations [30]. Generally, complexation, cation exchange, precipitation, electrostatic interactions, and chemical reduction represent the main metal sorption mechanisms. However, the role of each mechanism is variable for each metal. Li et al. [115] described the target mechanisms of As, Cr, Pb, Cd, and Hg in detail. On the other hand, sorption of ionisable and ionic organic compounds such as pharmaceuticals and pesticides on biochar-based sorbents is a more complex process and the relative contribution of each sub-mechanism is dependent on the type of sorbate, pH, and sorbent properties [116]. These authors suggested and characterized the main active processes in sorption of organic molecules from liquid media as nonspecific van der Waals force (exactly London dispersion force), solvophobic effect, H-bond, charge assisted H-bond, electron donor-acceptor interactions, electrostatic (coulombic) interactions, ligand exchange, Lewis acid–base reactions, covalent bond, and oxidative coupling.

6. Biochar for Microcystin Sorption Separation

The study of biochar application in the removal of various organic structures has illustrated the potential of this pyrogenic material in separation processes. The biochar boom in environmental technologies and agronomy raised the question of potential risk evaluation for MCs interaction with this pyrogenic carbonaceous material present in sediment/water environments [74]. While at the same time, Zhang et al. [29], Li et al. [27], and Liu et al. [28] revealed the efficiency of modified charcoal and biochar utilization as potential sorbents of MC-LR from aqueous solutions. In each case, existing knowledge gaps on sorption behaviour of cyanotoxins in contact with biochar limit widespread usage of this engineered waste-derived sorbent in water purification processes. Sorbents derived from biochar exhibit different structure and properties compared with activated carbon. Incomplete carbonization at low temperatures in the range of 300–700 °C and the absence of activation processes can bring new challenges in the characterization and subsequent application of biochar sorbents. The effect of feedstock and mineral composition can be crucial for sorption properties of pyrogenic carbonaceous material [27].

The mechanisms of sorption interactions between microcystin and biochar can be characterized by several potential processes such as electrostatic and hydrogen bonding, ion exchange, complexation, mesopore filling, hydrophobic interactions, and interactions with aromatic carbon (such as $\pi \pm \pi$ EDA and $\pi - \pi$ stacking) (Figure 3). $\Pi \pm \pi$ EDA represents $\pi \pm \pi$ electron donor–acceptor interactions between protonated guanidine groups of MCs and π-electron rich graphene surfaces of biochar [28]. $\Pi - \pi$ stacking is the main interaction between the benzene ring of MCs and aromatic units on biochar surfaces [74]. As mentioned previously, molecules of MCs have a more hydrophilic character with reactive carboxyl or guanidine functional groups. Therefore, the dominant mechanism of MCs sorption can be often attributed to hydrophobic interactions [74]. Liu et al. [28] reported that the hydrophobic leucine unit in a MC-LR molecule tends to be attracted to hydrophobic surfaces of giant reed-derived biochar via a hydrophobic interaction. The authors showed that the positive correlation between pyrolysis temperature and hydrophobic interactions, thus hydrophobicity, is a driving force in the sorption of MC-LR. Teixidó et al. [118] described sorption removal of hydrophilic sulfamethazine by biochar with electron donor–acceptor interaction between protonated aniline ring and on π-electrons rich carbon surface as the predominant driving force. However, this kind of interaction is not a major force during MCs interactions with biochar-based sorbents. Isolated π electron systems in the Adda side chain represent small fractions of the hydrophilic macromolecule.
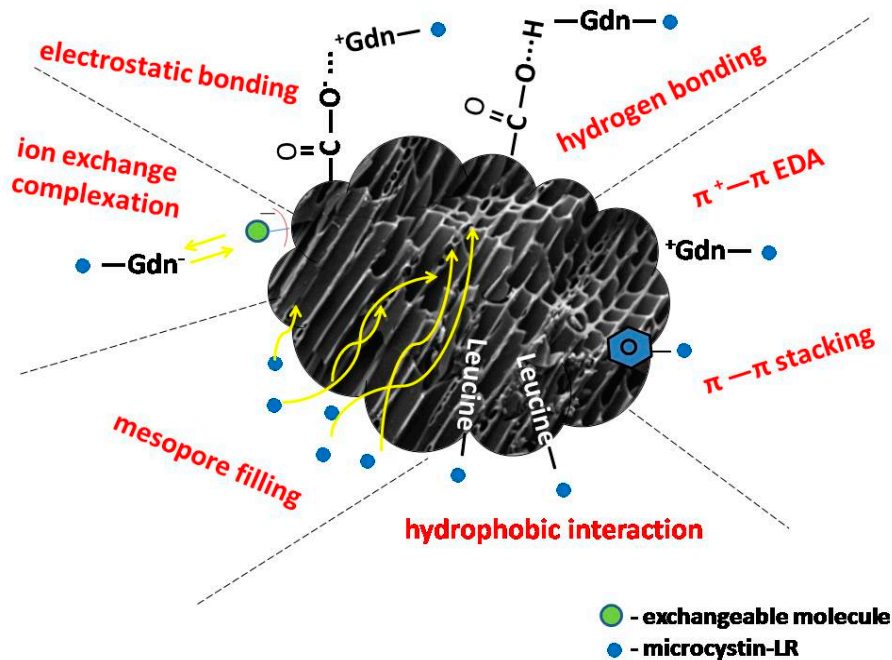

Figure 3. Suggested model of MC-LR sorption interactions with biochar-based sorbents.

On the other hand, Li et al. [74] showed how chemisorptions are the main force responsible for sorption of MC-LR molecules on wood-based biochar produced at 300 °C. Additionally, the authors confirmed physisorption and hydrogen bonding as the primary forces in sorption of MC-LR by the same biochar produced at 700 °C. One adsorbed MC-LR molecule can displace a considerable number of water molecules at the solid/liquid interface [119]. Thermodynamic calculations by Li et al. [74] demonstrated the ability of the MC-LR molecule to replace more water molecules on the biochar produced at lower temperatures. Li et al. [27] reported $\pi \pm \pi$ EDA interactions as the major driving forces of MC-LR sorption by biochars produced at 600 °C compared with biochars produced from the same feedstocks at 300 °C. Biochar produced at higher temperatures consists of highly aromatic structures providing larger π-electron-rich graphene sheets as electron donors.

The effect of porosity, as mentioned in Section 3, is crucial for sorption efficiency. According to Li et al. [27] and Zhang et al. [29], the three-dimensional size of the MC-LR molecule was determined

to be 1.9 nm × 1.5 nm × 1.1 nm, with a maximum length of 2.94 nm and width of 2.55 nm. Therefore, micropores represent inaccessible spaces for MC-LR molecules [27]. Biochars with lower surface area and lower concentration of mesopores can be less effective in sorption removal of MC-LR [74]. Liu et al. [28] showed that giant reed derived biochars produced at higher temperatures (>500 °C) have predominantly mesoporous structures and are thus more suited and effective in the removal of MC-LR from aqueous solutions.

The pH values of biochar and surface point of zero charge are further driving forces in the sorption mechanism of MCs. Biochars with lower pH, or under lower pH environmental conditions, can still contain minor surfaces with positive charges, thus columbic attraction between anionic microcystin molecules and sorbent can still be considered. The pH of the aquatic environment can severely influence the sorption efficiency of MCs. Generally speaking, sorption of these microbial toxins decreases with increasing pH of the environment. Sorption processes of MCs are inhibited by electrostatic repulsion between their mono oxoanionic species induced by increasing pH (2–4) and higher negative charge of biochar surfaces at pH 3–8 [28].

Additionally, molecules of MCs tend to coil under more acidic conditions, and thus sorption can be more effective. Higher pH provides higher concentrations of hydrophilic microcystin molecules and thus a higher tendency of MCs to remain in the aqueous environment rather than to interact with hydrophobic biochar-based sorbents. Wu et al. [120] confirmed this trend in MC-LR sorption by natural sediments, and Sathishkumar et al. [85] for MC-LR sorption by peats-derived sorbents. Ionisable functional groups of MCs and biochar surfaces can be easily protonated or deprotonated at different pH values. According to Li et al. [74], adsorption of MC-LR on biochars is attributed to the binding of MC-LR- anions to biochars with pH-dependent charges in aquatic systems. Liu et al. [28] found the highest sorption efficiency of MC-LR removal by giant reed-derived biochars at pH 3.5.

The sorption separation of MCs by biochar can also be influenced by competitive substances such as phosphates, citric acid, oxalic acid, and tannic acid, but with negligible effects from gallic acid, nitrates, and chlorides [74]. These authors suggested anion exchange as a possible contributing factor to MC-LR adsorption. Liu et al. [28] investigated the contribution of mineral composition to the overall sorption of MC-LR by giant reed-derived biochar. Their reported results revealed that mineral removal by deashing treatment barely impacts the adsorption of MC-LR by biochars produced at temperatures < 400 °C, whereas it significantly reduces sorption of MCs by biochars produced at temperatures > 400 °C.

Li et al. [74] showed adsorption irreversibility of MC-LR sorbed to wood-derived biochar and increased accumulation of MC-LR in biochar-amended sediments. The authors confirmed the associated risk of the undetermined prolonged fate of MC-LR in sediments and thus in aquatic environments. However, the benefits of high porosity, chemical stability, and significant sorption efficiency for removal processes of cyanotoxins can help guide the optimization of pyrolysis processes and the creation of a new class of so-called engineered or designed sorbents for water purification.

7. Conclusions

Elevated cyanotoxin concentrations in freshwater systems and drinking water sources following toxic cyanobacterial blooms require remediation to reduce risks to human and ecosystem health. Conventional methods for microcystin removal are insufficient or, as in the case of activated carbon, too expensive for widespread adoption. Alternative methods exist and have shown interesting results, but require continued research efforts. This review illustrates the potential of the pyrolysis process to inexpensively transform organic materials into efficient sorbents. In particular, biochar has proven effective as a sorbent for MCs in water thanks to its high porosity, chemical stability, and notable sorption efficiency. The physiochemical properties of a specifically engineered biochar for MCs remediation can be optimized through manipulating feedstock and pyrolysis conditions. Future research and product development for MCs sorption separation from contaminated aquatic environments can consider pyrolysed materials as attractive candidates. This work supports the continued exploration of inexpensive and feasible water remediation sorbents produced through

pyrolysis, but also demonstrates the need for further studies evaluating their effectiveness in the field under diverse conditions following harmful algal blooms worldwide.

References

1. Griffith, A.W.; Gobler, C.J. Harmful algal blooms: A climate change co-stressor in marine and freshwater ecosystems. *Harmful Algae* **2020**, *91*, 101590. [CrossRef]

2. Hoagland, P.; Anderson, D.M.; Kaoru, Y.; White, A.W. The economic effects of harmful algal blooms in the United States: Estimates, assessment issues, and information needs. *Estuaries* **2002**, *25*, 819–837. [CrossRef]

3. Harke, M.J.; Steffen, M.M.; Gobler, C.J.; Otten, T.G.; Wilhelm, S.W.; Wood, S.A.; Paerl, H.W. A review of the global ecology, genomics, and biogeography of the toxic cyanobacterium, *Microcystis* spp. *Harmful Algae* **2016**, *54*, 4–20. [CrossRef]

4. Wood, S.A.; Kelly, L.; Bouma-Gregson, K.; Humbert, J.F.; Laughinghouse IV, H.D.; Lazorchak, J.; McAllister, T.; McQueen, A.; Pokrzywinski, K.; Puddick, J.; et al. Toxic benthic freshwater cyanobacterial proliferations: Challenges and solutions for enhancing knowledge and improving monitoring and mitigation. *Freshw. Biol.* **2020**, *65*, 1824–1842. [CrossRef]

5. Codd, G.A.; Morrison, L.F.; Metcalf, J.S. Cyanobacterial toxins: Risk management for health protection. *Toxicol. Appl. Pharmacol.* **2005**, *203*, 264–272. [CrossRef] [PubMed]

6. Dodds, W.K.; Bouska, W.W.; Eitzmann, J.L.; Pilger, T.J.; Pitts, K.L.; Riley, A.J.; Schloesser, J.T.; Thornbrugh, D.J. Eutrophication of U. S. freshwaters: Analysis of potential economic damages. *Environ. Sci. Technol.* **2009**, *43*, 12–19. [CrossRef] [PubMed]

7. Paerl, H.W.; Huisman, J. Climate change: A catalyst for global expansion of harmful cyanobacterial blooms. *Environ. Microbiol. Rep.* **2009**, *1*, 27–37. [CrossRef] [PubMed]

8. Almanza, V.; Pedreros, P.; Laughinghouse IV, H.D.; Félez, J.; Parra, O.; Azocar, M.; Urrutia, R. Association between trophic state, watershed use and blooms of cyanobacteria in south-central Chile. *Limnologica* **2019**, *75*, 30–41. [CrossRef]

9. Huisman, J.; Codd, G.A.; Paerl, H.W.; Ibelings, B.W.; Verspagen, J.M.H.; Visser, P.M. Cyanobacterial blooms. *Nat. Rev. Microbiol.* **2018**, *16*, 471–483. [CrossRef]

10. Kust, A.; Řeháková, K.; Vrba, J.; Maicher, V.; Mareš, J.; Hrouzek, P.; Chiriac, M.C.; Benedová, Z.; Tesařová, B.; Saurav, K. Insight into Unprecedented Diversity of Cyanopeptides in Eutrophic Ponds Using an MS/MS Networking Approach. *Toxins* **2020**, *12*, 561. [CrossRef]

11. Carvalho, L.R.; Pipole, F.; Werner, V.R.; Laughinghouse IV, H.D.; Rangel, M.; Konno, K.; Camargo, A.C.M.; Sant'Anna, C.L. A Toxic Cyanobacterial Bloom in an Urban Coastal Lake, Rio Grande do Sul, Southern Brazil. *Braz. J. Microbiol.* **2008**, *39*, 761–769. [CrossRef] [PubMed]

12. Burford, M.A.; Carey, C.C.; Hamilton, D.P.; Huisman, J.; Paerl, H.W.; Wood, S.A.; Wulff, A. Perspective: Advancing the research agenda for improving understanding of cyanobacteria in a future of global change. *Harmful Algae* **2020**, *91*, 101601. [CrossRef]

13. Wells, M.L.; Karlson, B.; Wulff, A.; Kudela, R.; Trick, C.; Asnaghi, V.; Berdalet, E.; Cochlan, W.; Davidson, K.; De Rijcke, M.; et al. Future HAB science: Directions and challenges in a changing climate. *Harmful Algae* **2020**, *91*, 101632. [CrossRef] [PubMed]

14. Paerl, H.W.; Gardner, W.S.; Havens, K.E.; Joyner, A.J.; McCarthy, M.J.; Newell, S.E.; Qin, B.; Scott, J.D. Mitigating cyanobacterial harmful algal blooms in aquatic ecosystems impacted by climate change and anthropogenic nutrients. *Harmful Algae* **2016**, *54*, 213–222. [CrossRef]

15. Dawson, R.M. The toxicology of microcystins. *Toxicon* **1998**, *36*, 953–962. [CrossRef]

16. Shahmohamadloo, R.S.; Poirier, D.G.; Ortiz Almirall, X.; Bhavsar, S.P.; Sibley, P.K. Assessing the toxicity of cell-bound microcystins on freshwater pelagic and benthic invertebrates. *Ecotoxicol. Environ. Saf.* **2020**, *188*, 109945. [CrossRef]

17. IARC. *Ingested Nitrate and Nitrite, and Cyanobacterial Peptide Toxins/IARC Monographs on the Evaluation of Carcinogenic Risks to Humans Volume 94*; IARC: Lyon, France, 2010.

18. WHO. *Guidelines for Drinking-Water Quality: Fourth Edition Incorporating the First Addendum*; WHO: Geneva, Switzerland, 2017.

19. Park, J.A.; Jung, S.M.; Choi, J.W.; Kim, J.H.; Hong, S.; Lee, S.H. Mesoporous carbon for efficient removal of microcystin-LR in drinking water sources, Nak-Dong River, South Korea: Application to a field-scale drinking water treatment plant. *Chemosphere* **2018**, *193*, 883–891. [CrossRef]

20. Ho, L.; Lambling, P.; Bustamante, H.; Duker, P.; Newcombe, G. Application of powdered activated carbon for adsorption of cylindrospermopsin and microcystin toxins from drinking water supplies. *Water Res.* **2011**, *45*, 2954–2964. [CrossRef]

21. Falconer, I.R.; Runnegar, M.T.C.; Buckley, T.; Huyn, L.; Bradshaw, P. Using activated carbon to remove toxicity from drinking water containing cyanobacterial blooms. *J. Am. Water Work. Assoc.* **1989**, *81*, 102–106. [CrossRef]

22. Mashile, P.P.; Mpupa, A.; Nomngongo, P.N. Adsorptive removal of microcystin-LR from surface and wastewater using tyre-based powdered activated carbon: Kinetics and isotherms. *Toxicon* **2018**, *145*, 25–31. [CrossRef]

23. Roegner, F.A.; Brena, B.; González-Sapienza, G.; Puschner, B. Microcystins in potable surface waters: Toxic effects and removal strategies. *J. Appl. Toxicol.* **2014**, *34*, 441–457. [CrossRef]

24. Basu, P. *Pyrolysis, in: Biomass Gasification, Pyrolysis and Torrefaction: Practical Design and Theory*; Elsevier: Amsterdam, The Netherlands, 2018; pp. 155–187.

25. Wang, J.; Wang, S. Preparation, modification and environmental application of biochar: A review. *J. Clean. Prod.* **2019**, *227*, 1002–1022. [CrossRef]

26. Ahmed, M.J.; Hameed, B.H. Insight into the co-pyrolysis of different blended feedstocks to biochar for the adsorption of organic and inorganic pollutants: A review. *J. Clean. Prod.* **2020**, *265*, 121762. [CrossRef]

27. Li, J.; Cao, L.; Yuan, Y.; Wang, R.; Wen, Y.; Man, J. Comparative studz for microcystin-LR sorption onto biochars produced from various plant-and animal-wastes at different pyrolysis temperatures: Influencing mechanisms of biochar properties. *Bioresour. Technol.* **2018**, *247*, 794–803. [CrossRef] [PubMed]

28. Liu, G.; Zheng, H.; Zhai, X.; Wang, Z. Characteristics and mechanisms of microcystin/LR adsorption by giant reed-derived biochars: Role of minerals, pores and functional groups. *J. Clean. Prod.* **2018**, *176*, 463–473. [CrossRef]

29. Zhang, H.; Zhu, G.; Jia, X.; Ding, Y.; Zhang, M.; Gao, Q.; Hu, C.; Xu, S. Removal of microcystin-LR from drinking water using a bamboo-based charcoal adsorbents modified with chitosan. *J. Environ. Sci.* **2011**, *23*, 1983–1988. [CrossRef]

30. Li, J.M.; Li, R.H.; Li, J. Current research scenario for microcystins biodegradation—A review on fundamental knowledge, application prospects and challenges. *Sci. Total Environ.* **2017**, *595*, 615–632. [CrossRef]

31. Spoof, L.; Catherine, A. Tables of microcystins and nodularins, Appendix 3. In *Handbook of Cyanobacterial Monitoring and Cyanotoxin Analysis*, 1st ed.; Meriluoto, J., Spoof, L., Cold, G.A., Eds.; John Wiley and Sons, Ltd.: Hoboken, NJ, USA, 2017.

32. Turner, A.D.; Dhanji-Rapkova, M.; OŃeill, A.; Coates, L.; Lewis, A.; Lewis, K. Analysis of microcystins in cyanobacterial blooms from freshwater bodies in England. *Toxins* **2018**, *10*, 39. [CrossRef] [PubMed]

33. Merel, S.; Clement, M.; Thomas, O. State of the art on cyanotoxins in water and their behaviour towards chlorine. *Toxicon* **2010**, *55*, 677–691. [CrossRef]

34. Trinchet, I.; Cadel-Six, S.; Djediat, C.; Marie, B.; Bernard, C.; Puiseux-Dao, S.; Krys, S.; Edery, M. Toxicity of harmful cyanobacterial blooms to bream and roach. *Toxicon* **2013**, *71*, 121–127. [CrossRef]

35. Humpage, R.; Hardy, S.J.; Moore, E.J.; Froscio, S.M.; Falconer, I.R. Microcystins (cyanobacterial toxins) in drinking water enhance the growth of aberrant cryptfoci in the mouse colon. *J. Toxicol. Environ. Health A* **2000**, *61*, 155–165. [PubMed]

36. Tillett, D.; Dittmann, E.; Erhard, M.; von Dohren, H.; Borner, T.; Neilan, B.A. Structural organization of microcystin biosynthesis in Microcystis aeruginosa PCC7806: An integrated peptide-polyketide synthetase systém. *Chem. Biol.* **2000**, *7*, 753–764. [CrossRef]

37. Mazur-Marzec, H.; Plinski, M. Do toxic cyanobacteria blooms pose a threat to the Baltic ecosystem? *Oceanologia* **2009**, *51*, 293–319. [CrossRef]

38. Jones, G.J.; Falconer, I.R.; Wilkins, R.M. Persistence of cyclic peptide toxins in dried Microcystis aeruginosa crusts from lake Mokoan, Australia. *Environ. Toxicol. Water Qual.* **1995**, *10*, 19–24. [CrossRef]

39. Schmidt, J.R.; Wilhelm, S.W.; Boyer, G.L. The Fate of Microcystins in the Environment and Challenges for Monitoring. *Toxins* **2014**, *6*, 3354–3387. [CrossRef]

40. Boopathi, T.; Ki, J.S. Impact of environmental factors on the regulation of cyanotoxin production. *Toxins* **2014**, *6*, 1951–1978. [CrossRef]

41. Žegura, B.; Štraser, A.; Filipič, M. Genotoxicity and potential carcinogenicity of cyanobacterial toxins–A review. *Mutat. Res. Rev. Mutat.* **2011**, *727*, 16–41. [CrossRef]

42. Fischer, A.; Hoeger, S.J.; Stemmer, K.; Feurstein, D.J.; Knobeloch, D.; Nussler, A.; Dietrich, D.R. The role of organic anion transporting polypeptides (OATPs/SLCOs) in the toxicity of different microcystin congeners in vitro: A comparison of primary human hepatocytes and OATP-transfected HEK293 cells. *Toxicol. Appl. Pharmacol.* **2010**, *245*, 9–20. [CrossRef]

43. Frangez, R.; Zuzek, M.C.; Mrkun, J.; Suput, D.; Sedmak, B.; Kosec, M. Microcystin-LR affects cytoskeleton and morphology of rabbit primary whole embryo cultured cells in vitro. *Toxicon* **2003**, *41*, 999–1005. [CrossRef]

44. Davis, M.A.; Chang, S.H.; Trump, B.F. Differential sensitivity of normal and H-ras Oncogene-transformed rat kidney epithelial cells to okadaic acid-induced apoptosis. *Toxicol. Appl. Pharmacol.* **1996**, *141*, 93–101. [CrossRef]

45. Ding, W.X.; Nam-Ong, C. Role of oxidative stress and mitochondrial changes in cyanobacteria-induced apoptosis and hepatotoxicity. *FEMS Microbiol. Lett.* **2003**, *220*, 1–7. [CrossRef]

46. Žegura, B.; Volcic, M.; Lah, T.T.; Filipic, M. Different sensitivities of human colon adenocarcinoma (CaCo-2), astrocytoma (IPDDC-A2) and lymphoblastoid (NCNC) cell lines to microcystin-LR induced reactive oxygen species and DNA damage. *Toxicon* **2008**, *52*, 518–525. [CrossRef] [PubMed]

47. Westrick, J.A.; Szlag, D.C.; Southwell, B.J.; Sinclair, J. A review of cyanobacteria and cyanotoxins removal/inactivation in drinking water treatment. *Anal. Bioanal. Chem.* **2010**, *397*, 1705–1714. [CrossRef] [PubMed]

48. Teixeira, M.R.; Rosa, M.J.; Sorlini, S.; Biasibetti, M.; Christophoridis, C. Removal of Cyanobacteria and Cyanotoxins by Conventional Physical-chemical Treatment. In *Water Treatment for Purification from Cyanobacteria and Cyanotoxins*; Hiskia, A.E., Triantis, T.M., Antoniou, M.G., Kaloudis, T., Dionysiou, D.D., Eds.; Wiley: Hoboken, NJ, USA, 2020; pp. 69–98.

49. Feitz, A.J.; Waite, T.D.; Jones, G.J.; Boyden, B.H.; Orr, P.T. Photocatalytic degradation of the blue green algal toxin microcystin-LR in a natural organic-aqueous matrix. *Environ. Sci. Technol.* **1999**, *33*, 243–249. [CrossRef]

50. Gurbuz, F.; Codd, G.A. Microcystin removal by a natural-occuring substance: Pumice. *Bull. Environ. Contam. Toxicol.* **2008**, *81*, 323–327. [CrossRef] [PubMed]

51. Teixeira, M.R.; Rosa, M.J. Comparing dissolved air flotation and conventional sedimentation to remove cyanobacterial cells of Microcystis aeruginosa Part II. The effect of water background organics. *Sep. Purif. Technol.* **2007**, *53*, 126–134. [CrossRef]

52. Crossley, I.A.; Valade, M.T. A review of the technological developments of dissolved air flotation. *J. Water Supply Res. Technol.* **2006**, *55*, 479–491. [CrossRef]

53. Laszakovits, J.; MacKay, A.A. Removal of cyanotoxins by potassium permanganate: Incorporating competition from natural water constituents. *Water Res.* **2019**, *155*, 86–95. [CrossRef]

54. Kinley-Baird, C.; Calomeni, A.; Berthold, D.E.; Lefler, F.W.; Barbosa, M.; Rodgers, J.H.; Laughinghouse, H.D., IV. Laboratory-scale evaluation of effectiveness for control of microcystin producing cyanobacteria from Lake Okeechobee, Florida (USA). *Ecotoxicol. Environ. Saf.* **2021**, *207*, 111233. [CrossRef]

55. Kinley, C.M.; Iwinski-Wood, K.J.; Geer, T.D.; Hendrikse, M.; McQueen, A.D.; Calomeni, A.J.; Liang, J.; Friesen, V.; Simair, M.C.; Rodgers, J.H. Microcystin-LR degradation following copper-based algaecide exposures. *Water Air Soil Pollut.* **2018**, *229*, 62. [CrossRef]

56. Jones, G.J.; Orr, P.T. Release and degradation of microcystin following algicide treatment of a *Microcystis aeruginosa* bloom in a recreational lake, as determined by HPLC and protein phosphatase inhibition assay. *Water Res.* **1994**, *28*, 871–876. [CrossRef]

57. Brooke, S.; Newcombe, G.; Nicholson, B.; Klass, G. Decrease in toxicity of microcystins LA and LR in drinking water by ozonation. *Toxicon* **2006**, *48*, 1054–1059. [CrossRef] [PubMed]

58. Ho, L.; Sawade, E.; Newcombe, G. Biological treatment options for cyanobacteria metabolite removal—A review. *Water Res.* **2012**, *46*, 1536–1548. [CrossRef] [PubMed]

59. Lawton, L.A.; Robertson, P.K.J. Physico-chemical treatment methods for the removal of microcystins (cyanobacterial hepatotoxins) from potable waters. *Chem. Soc. Rev.* **1999**, *28*, 217–224. [CrossRef]

60. Vlad, S.; Anderson, W.B.; Peldszus, S.; Huck, P.M. Removal of the cyanotoxin anatoxin-a by drinking water treatment processes: A review. *J. Water Health* **2014**, *12*, 601–617. [CrossRef] [PubMed]

61. Pavagadhi, S.; Tang, A.L.L.; Sathishkumar, M.; Loh, K.P.; Balasubramanian, R. Removal of microcystin-LR and microcystin-RR by graphene oxide: Adsorption and kinetic experiments. *Water Res.* **2013**, *47*, 4621–4629. [CrossRef] [PubMed]

62. Wang, X.L.; Xing, B.S. Sorption of organic contaminants by biopolymer-derived chars. *Environ. Sci. Technol.* **2007**, *41*, 8342–8348. [CrossRef]

63. Hena, S.; Ismail, N.; Isaam, A.M.; Ahmad, A.; Bhawani, S.A. Removal of microcystin-LR from agueous solutions using % burn-off activated carbon of waste wood material. *J. Water Supply Res. Technol.* **2014**, *63*, 332–341. [CrossRef]

64. Pendleton, P.; Schumann, R.; Wong, S.H. Microcystin adsorption by activated carbon. *J. Collod. Interf. Sci.* **2001**, *240*, 1–8. [CrossRef]

65. Teng, W.; Wu, Z.; Fan, J.; Zhang, W.X.; Zhao, D. Amino-functionalized ordered mesoporous carbon for the separation of toxic microcystin-LR. *J. Mat. Chem. A* **2015**, *3*, 19168. [CrossRef]

66. Newcombe, G.; Morrison, J.; Hepplewhite, C.; Knappe, D.R.U. Simultaneous adsorption of MIB and NOM onto activated carbon. II. Competitive effects. *Carbon* **2002**, *40*, 2147–2156. [CrossRef]

67. Ho, L.; Newcombe, G. Evaluating the adsorption of microcystin toxins using granular activated carbon (GAC). *J. Water Supply Res. Technol.* **2007**, *56*, 281–291. [CrossRef]

68. Hnatukova, P.; Kopecka, I.; Pivokonsky, M. Adsorption of cellular peptides of Microcystis aeruginosa and two herbicides onto activated carbon: Effect of surface charge and interactions. *Water Res.* **2011**, *45*, 3359–3368. [CrossRef] [PubMed]

69. Huang, W.J.; Cheng, B.L.; Cheng, Y.L. Adsorption of microcystin-LR by three types of activated carbon. *J. Hazard. Mater.* **2007**, *141*, 115–122. [CrossRef]

70. Campinas, M.; Rosa, M.J. Assessing PAC contribution to the NOM fouling control in PAC/UF systems. *Water Res.* **2010**, *44*, 1636–1644. [CrossRef] [PubMed]

71. Drogui, P.; Daghrir, R.; Simard, M.C.; Sauvageau, C.; Blais, J.F. Removal of microcystin-LR from spiked water using either activated carbon or anthracite as filter material. *Environ. Technol.* **2012**, *33*, 381–391. [CrossRef]

72. Zhi, M.; Yang, F.; Meng, F.; Li, M.; Manivannan, A.; Wu, N. Effects of pore structure on performance of an activated-carbon supercapacitor electrode recycled from scrap waste tires. *ACS Sustain. Chem. Eng.* **2014**, *2*, 1592–1598. [CrossRef]

73. Lou, F.; Zhou, H.; Tran, T.D.; Buan, M.E.M.; Vullum-Bruer, F.; Ronning, M.; Walmsley, J.C.; Chen, D. Coaxial carbon/metal oxide/aligned carbon nanotube arrays as high-performance anodes for lithium ion batteries. *ChemSusChem* **2014**, *7*, 1335–1346. [CrossRef]

74. Li, L.; Qiu, Y.; Huang, J.; Li, F.; Sheng, G.D. Mechanisms and factors influencing adsorption of microcystin-LR on biochars. *Water Air Soil Poll.* **2014**, *225*, 2220. [CrossRef]

75. Kim, S.; Yun, Y.S.; Choi, Y.E. Development of waste biomass based sorbent for removal of cyanotoxin microcystin-LR from aqueous phases. *Bioresource Technol.* **2018**, *247*, 690–696. [CrossRef]

76. Yasmin, R.; aftab, K.; Kashif, M. Removal of microcystin-LR from agueous solution using *Moringa oleifera* Lam. Seeds. *Water Sci. Technol.* **2019**, *79*, 104–113. [CrossRef] [PubMed]

77. Sathya, K.; Saranya, P.; Swarnalatha, S.; Mandal, A.; Sekaran, G. Removal of microcystin-RR, a membrane foulant using exocellular polymer from *Enterobacter ludwigii*: Kinetic and isotherm studies. *Desalination* **2015**, *369*, 175–187.

78. Park, J.H.; Wang, J.J.; Kim, S.H.; Kang, S.W.; Jeong, C.Y.; Jeon, J.R.; Park, H.P.; Cho, J.S.; Delaune, R.D.; Seo, D.C. Cadmium adsorption characteristics of biochars derived using various pine t tree residues and pyrolysis temperatures. *J. Colloid Interface Sci.* **2019**, *553*, 298–307. [CrossRef] [PubMed]

79. Frišták, V.; Pipíška, M.; Soja, G. Pyrolysis treatment of sewage sludge: A promising way to produce phosphorus fertilizer. *J. Clean. Prod.* **2018**, *172*, 1772–1778. [CrossRef]

80. Morris, R.J.; Williams, D.E.; Luu, H.A.; Holmes, C.F.; Andersen, R.J.; Calvert, S.E. The adsorption of microcystin-LR by natural clay particles. *Toxicon* **2000**, *38*, 303–308. [CrossRef]

81. Laughinghouse IV, H.D.; Lefler, F.W.; Berthold, D.E.; Bishop, W.M. Sorption of microcystin using lanthanum-modified bentonite clay. *J. Aquat. Plant Manag.* **2020**, *58*, 72–75.

82. Wang, Z.; Wang, C.; Wang, P.; Qian, J.; Hou, J.; Ao, Y. Process optimization for microcystin-LR adsorption onto nano-sized montmorillonite K10: Application of response surface methodology. *Water Air Soil Poll.* **2014**, *225*, 2124. [CrossRef]

83. Wang, Z.; Wang, C.; Wang, P.; Qian, J.; Hou, J.; Ao, Y. Response surface modelling and optimization of microcystin-LR remocal from agueous phase by polyacrylamide/sodium alginate-motmorillonite superabsorbent nanocomposite. *Desal. Eater Treat.* **2015**, *56*, 1121–1139. [CrossRef]

84. Akbal, F.O.; Akdemir, N.; Onar, A.N. FT-IR spectroscopic detection of pesticide after sorption onto modified pumice. *Talanta* **2000**, *53*, 131–135. [CrossRef]

85. Sathishkumar, M.; Pavagadhi, S.; Vijayaraghavan, K.; Balasubramanian, R.; Ong, S.L. Concomitant uptake of microcystin-LR and -RR by peat under various environmental conditions. *Chem. Eng. J.* **2011**, *172*, 754–762. [CrossRef]

86. Lee, J.; Walker, H.W. Adsorption of microczstin-LR onto iron oxide nanoparticles. *Colloid. Surface A* **2011**, *373*, 94–100. [CrossRef]

87. Okupnik, A.; Contardo-Jara, V.; Pflugmacher, S. Potential role of engineered nanoparticles as contaminant carriers in aquatic ecosystems: Estimating sorption processes of the cyanobacterial toxin microcystin-LR by TiO_2 nanoparticles. *Colloid. Surface A* **2015**, *481*, 460–467. [CrossRef]

88. Wu, L.; Lan, J.; Wang, S.; Zhu, J. Synthesis of N-doped carbon xerogel (N-CX) and its applications for adsorption removal of microcystin-LR. *Z. Phys. Chem.* **2017**, *231*, 1525–1541. [CrossRef]

89. EBC. *European Biochar Certificate-Guidelines for a Sustainable Production of Biochar*; EBC: Arbaz, Switzerland, 2015. [CrossRef]

90. Shaheen, S.M.; Niazi, N.K.; Hassan, N.E.E.; Bibi, I.; Wang, H.; Tsang, D.C.W.; Ok, Y.S.; Bolan, N.; Rinklebe, J. Wood-based biochar for the removal of potentially toxic elements in weter and wastewater: A critical review. *Int. Mater. Rev.* **2019**, *64*, 216–247. [CrossRef]

91. Micháleková-Richveisová, B.; Frišták, V.; Pipíška, M.; Duriška, L.; Moreno-Jimenez, E.; Soja, G. Iron-impregnated biochars as effective phosphate sorption materials. *Environ. Sci. Pollut. Res. Int.* **2017**, *24*, 463–475. [CrossRef]

92. Bridgwater, A.V. Review of fast pyrolysis of biomass and product upgrading. *Biomass Bioenergy* **2012**, *38*, 68–94. [CrossRef]

93. Kunhikrishnan, A.; Bibi, I.; Bolan, N.; Seshadri, B.; Choppala, G.; Niazi, N.K.; Kim, W.I.; Ok, Y.S.; Uchimiya, S.M.; Chang, S.; et al. Biochar for inorganic contaminant management in waste and wastewater. In *Biochar: Production, Characterization and Applications*; CRC Press: Boca Raton, FL, USA, 2015; pp. 167–219.

94. Brown, R.A.; Kercher, A.K.; Nguyen, T.H.; Nagle, D.C.; Ball, W.P. Production and characterization of synthetic wood chars for use as surrogates for natural sorbents. *Org. Geochem.* **2006**, *37*, 321–333. [CrossRef]

95. Rutherford, D.W.; Wershaw, R.L.; Cox, L.G. *Changes in Composition and Porosity Occurring during the Thermal Degradation of Wood and Wood Components*; US Geological Survey, Scientific Investigation Report 2004-5292; USGS: Reston, VA, USA, 2004.

96. Mohan, D.; Pittman, C.U.; Steele, P.H. Pyrolysis of wood/biomass for bio-oil: A critical review. *Energy Fuels* **2006**, *20*, 848–889. [CrossRef]

97. Lehmann, J.; Joseph, S. *Biochar for Environmental Management—Science, Technology and Implementation*, 2nd ed.; Routledge: London, UK; Sterling, VA, USA, 2015.

98. Park, S.H.; Cho, H.J.; Ryu, C.; Park, Y.K. Removal of copper (II) in aqueous solution using pyrolytic biochars derived from red macroalga *Porphyra tenera*. *J. Ind. Eng. Chem.* **2016**, *36*, 314–319. [CrossRef]

99.   Zhang, R.H.; Li, Z.G.; Liu, X.D.; Wang, B.C.; Zhou, G.L.; Huang, X.X.; Lin, C.F.; Wang, A.H.; Brooks, M. Immobilization and bioavailability of heavy metals in greenhouse soils amended with rice straw-derived biochar. *Ecol. Eng.* **2017**, *98*, 183–188. [CrossRef]

100.   Bogusz, A.; Oleszczuk, P.; Dobrowolski, R. Application of laboratory prepared and commercially available biochars to adsorption of cadmium, copper and zinc ions from water. *Bioresour. Technol.* **2015**, *196*, 540–549. [CrossRef] [PubMed]

101.   Ma, Y.; Liu, W.J.; Zhang, N.; Li, Y.S.; Jiang, H.; Sheng, G.P. Polyethylenimine modified biochar adsorbent for hexavalent chromium removal from the aqueous solution. *Bioresour. Technol.* **2014**, *169*, 403–408. [CrossRef]

102.   Agrafioti, E.; Kalderis, D.; Diamadopoulos, E. Ca and Fe modified biochars as adsorbents of arsenic and chromium in aqueous solutions. *J. Environ. Manag.* **2014**, *146*, 444–450. [CrossRef] [PubMed]

103.   Inyang, M.; Gao, B.; Yao, Y.; Xue, Y.; Zimmerman, A.R.; Pullammanappallil, P.; Cao, X. Removal of heavy metals from aqueous solution by biochars derived from anaerobically digested biomass. *Bioresour. Technol.* **2012**, *110*, 50–56. [CrossRef]

104.   Tang, L.; Yu, J.; Pang, Y.; Zeng, G.; Deng, Y.; Wang, J.; Ren, X.; Ye, S.; Peng, B.; Feng, H. Sustainable efficient adsorbent: Alkali-acid modified magnetic biochar derived from sewage sludge for aqueous organic contaminant removal. *Chem. Eng. J.* **2018**, *336*, 160–169. [CrossRef]

105.   Ruthiraan, M.; Abdullah, E.C.; Mubarak, N.M.; Noraini, M.N. A promising route of magnetic based materials for removal of cadmium and methylene blue from waste water. *J. Environ. Chem. Eng.* **2017**, *5*, 1447–1455. [CrossRef]

106.   Lin, L.; Jiang, W.; Xu, P. Comparative study on pharmaceuticals adsorption in reclaimed water desalination concentrate using biochar: Impact of salts and organic matter. *Sci. Total Environ.* **2017**, *601*, 857–864. [CrossRef]

107.   Tan, X.; Liu, Y.; Gu, Y.; Xu, Y.; Zeng, G.M.; Hu, X.J.; Liu, S.B.; Wang, X.; Liu, S.M.; Li, J. Biochar-based nano-composites for the decontamination of wastewater: A review. *Bioresour. Technol.* **2016**, *212*, 318–333. [CrossRef] [PubMed]

108.   Rajapaksha, A.U.; Chen, S.S.; Tsang, D.C.; Zhang, M.; Vithanage, M.; Mandal, S.; Gao, B.; Bolan, N.S.; Ok, Y.S. Engineered/designer biochar for contaminant removal/immobilization from soil and water: Potential and implication of biochar modification. *Chemosphere* **2016**, *148*, 276–291. [CrossRef]

109.   Igalavithana, A.D.; Lee, S.E.; Lee, Y.H.; Tsang, D.C.W.; Rinklebe, J.; Kwon, E.E.; Ok, Y.S. Heavy metal immobilization and microbial community abundance by vegetable waste and pine cone biochar of agricultural soils. *Chemosphere* **2017**, *174*, 593–603. [CrossRef]

110.   Dieguez-Alonso, A.; Anca-Couce, A.; Frišták, V.; Moreno-Jiménez, E.; Bacher, M.; Bucheli, T.D.; Cimò, G.; Conte, P.; Hagemann, N.; Haller, A.; et al. Designing biochar properties through the blending of biomass feedstock with metals: Impact on oxyanions adsorption behavior. *Chemosphere* **2019**, *214*, 743–753. [CrossRef] [PubMed]

111.   Zama, E.F.; Zhu, Y.G.; Reid, B.J.; Sun, G.X. The role of biocharproperties in influencing the sorption and desorption of Pb(II), Cd(II) and As(III) in aqueous solution. *J. Clean Prod.* **2017**, *148*, 127–136. [CrossRef]

112.   Jiang, J.; Pang, S.Y.; Ma, J. Comment on Adsorption of hydroxyl-and amino-substituted aromatics on carbon nanotubes. *Environ. Sci. Technol.* **2009**, *43*, 2–3. [CrossRef] [PubMed]

113.   Kloss, S.; Zehetner, F.; Oburger, E.; Buecker, J.; Kitzler, B.; Wenzel, W.W.; Wimmer, B.; Soja, G. Trace element concentrations in leachates and mustard plant tissue (*Sinapis alba* L.) after biochar application to temperate soils. *Sci. Total Environ.* **2014**, *481*, 498–508. [CrossRef] [PubMed]

114.   Frišták, V.; Micháleková-Richveisová, B.; Víglašová, E.; Ďuriška, L.; Galamboš, M.; Moreno-Jimenéz, E.; Pipíška, M.; Soja, G. Sorption separation of Eu and As from single-component systems by Fe-modified biochar: Kinetic and equilibrium study. *J. Iran. Chem. Soc.* **2017**, *14*, 521–530. [CrossRef]

115.   Li, X.; Pignatello, J.J.; Wang, Y.; Xing, B. New insight into adsorption mechanism of ionizable compounds on carbon nanotubes. *Environ. Sci. Technol.* **2013**, *47*, 8334–8341. [CrossRef]

116.   Kah, M.; Sigmund, G.; Xiao, F.; Hofmann, T. Sorption of ionizable and ionic organic compounds to biochar, activated carbon and other carbonaceous materials. *Water Res.* **2017**, *124*, 673–692. [CrossRef]

117.   Sizmur, T.; Fresno, T.; Akgül, G.; Frost, H.; Moreno-Jiménez, E. Biochar modification to enhance sorption of inorganics from water- review. *Bioresour. Technol.* **2018**, *246*, 34–47. [CrossRef]

118.   Teixidó, M.; Pignatello, J.J.; Beltrán, J.L.; Granados, M.; Peccia, J. Speciation of the ionizable antibiotic sulfamethazine on black carbon (biochar). *Environ. Sci. Technol.* **2011**, *45*, 10020–10027. [CrossRef]

119. Lin, Y.R.; Teng, H.S. Mesoporous carbons from waste tire char and their application in wastewater discoloration. *Micropor. Mesopor. Mat.* **2002**, *54*, 167–174. [CrossRef]

120. Wu, X.Q.; Xiao, B.D.; Li, R.H.; Wang, C.B.; Huang, J.T.; Wang, Z. Mechanisms and factors affecting sorption of microcystins onto natural sediments. *Environ. Sci. Technol.* **2011**, *45*, 2641–2647. [CrossRef]

Publisher's Note: MDPI stays neutral with regard to jurisdictional claims in published maps and institutional affiliations.